High-Performance Liquid-Catalyst Fuel Cell for Direct Biomass-into-Electricity Conversion**

Wei Liu, Wei Mu, and Yulin Deng*

Abstract: *Herein, we report high-performance fuel cells that are catalyzed solely by polyoxometalate (POM) solution without any solid metal or metal oxide. The novel design of the liquid-catalyst fuel cells (LCFC) changes the traditional gas–solid-surface heterogeneous reactions to liquid-catalysis reactions. With this design, raw biomasses, such as cellulose, starch, and even grass or wood powders can be directly converted into electricity. The power densities of the fuel cell with switchgrass (dry powder) and bush allamanda (freshly collected) are 44 mW cm^{-2} and 51 mW cm^{-2} respectively. For the cellulose-based biomass fuel cell, the power density is almost 3000 times higher than that of cellulose-based microbial fuel cells. Unlike noble-metal catalysts, POMs are tolerant to most organic and inorganic contaminants. Therefore, almost any raw biomass can be used directly to produce electricity without prior purification.*

Fuel cells present a key technology for power generation with high-energy yield and low environmental impact. The direct hydrogen- or alcohol-based proton-exchange membrane fuel cells (PEMFC) have been studied for decades. Noble-metal catalysts are intensively used in PEMFC owing to its capability to not only catalyze fuel oxidation at the anode but also accelerate the oxygen-reduction reaction (ORR) at the cathode.[1] However, noble-metal electrodes have several intrinsic disadvantages. The noble-metal (e.g. Pt, Ru, Pd) catalyst is very expensive, accounting for approximately 80% of the total cost of a PEMFC.[2] In addition, the noble-metal catalysts show low tolerance to the impurities present in fuels, even in trace amounts.[1] Therefore, the fuel-purification process adds additional cost. Moreover, the noble metal is not able to effectively cleave C−C bonds in fuels at low temperature.[3] As a result, the output power and efficiency dramatically drops when fueled with higher alcohols.[4] For these reasons, natural polymeric biomass, such as starch, cellulose, grass and wood powders, cannot be directly

used as fuel in a conventional low-temperature PEMFC. Non-noble-metal electrocatalysts, such as iron[5] or cobalt,[6] have been studied extensively. However, these catalysts have not been able to completely substitute the current noble-metal catalysts.

Biomass can provide a significant fraction of the renewable energy and can re-grow over a relatively short period of time. Using biomass energy can decrease carbon dioxide emission and reduce the impact on global warming. Biomass can either be used by combustion to produce thermal energy directly or by conversion to biofuels to indirectly produce thermal energy. However, owing to the lack of an effective catalyst, it is very difficult to directly convert biomass into electricity without high-temperature combustion. The solid-oxide fuel cell (SOFC) and microbial fuel cell (MFC) have been developed to reduce the dependence on noble-metal catalysts and both cells can use lignocellulosic biomass-derived fuels.[7] However, the conventional SOFC requires very high operating temperatures (500–1000°C) to gasify the biomass fuels, and is highly vulnerable to carbon buildup (coking) and sulfur-contaminants.[8] Microbial fuel cells use enzymes or microorganisms to decompose biomass, but the low electric power output, high chemo-selectivity for substrates, rigorous reaction conditions and limited lifetime seriously hinder their applications.[9]

Recently, we reported a novel solar-induced hybrid fuel cell which can directly consume biomass without chemical pretreatment.[10] The work demonstrated that polyoxometalates (POMs) could function as a photo-catalyst and charge carrier to realize a new pathway for direct biomass-into-electricity conversion. Herein, we report a 3D electrode-based fuel cell that mediated by liquid catalyst and has a high power output improvement.

The liquid-catalyst fuel cell (LCFC) reported herein is completely noble-metal free. Two POM solutions with different redox potentials were utilized in this fuel cell: one oxidizes biomass either under sunlight or heating in an anode tank and the other reacts with the oxygen at the cathode. The cell is schematically shown in Figure 1A. It was constructed using a Nafion 115 membrane sandwiched between two 3D graphite electrodes with no metal loading (detail of electrodes is shown in Figure S1 of the Supporting Information). The POM-**I** ($H_3PW_{11}MoO_{40}$) solution, along with the biomass, was stored in the anode electrolyte tank. The oxidation of biomass fuel occurred in the anode electrolyte solution (left of Figure 1A) under either sunlight irradiation or direct heating. The reduced POM solution cyclically pumped through the anode. As shown on the right side of Figure 1A, a non-Keggin-type $H_{12}P_3Mo_{18}V_7O_{85}$ aqueous solution (noted as POM-**II**) was stored in the cathode tank. The regeneration
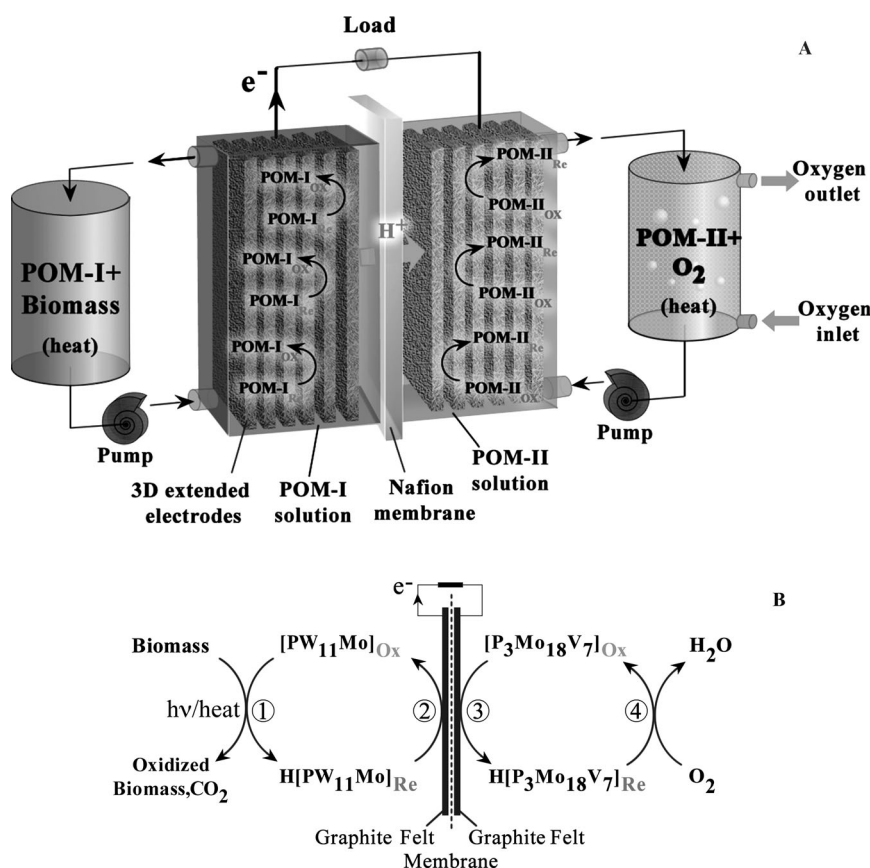
[*] W. Liu,[+] W. Mu,[+] Prof. Dr. Y. Deng
School of Chemical & Biomolecular Engineering and RBI at Georgia Tech, Georgia Institute of Technology
500 10th Street N.W., Atlanta, GA 30332-0620 (USA)
E-mail: yulin.deng@chbe.gatech.edu
W. Liu[+]
College of Chemistry and Chemical Engineering
Hunan University (China)

[+] These authors contributed equally to this work.

Figure 1. A) Schematic illustration of the direct biomass fuel cell coupled with biomass-POM-I solution anode tank and POM-II-oxygen cathode tank. B) General pathway of redox reactions in this fuel cell, see text for details. The subscript Re refers to the reduced form of the POM and Ox refers to the oxidized form.

density (based on unit area of membrane) can be significantly improved. Clearly, the conventional fuel cell design cannot make use of this advantage.

The entire redox reaction pathway of biomass, oxygen, and both POMs includes four major steps, as shown in Figure 1 B. In the step 1, oxidation of biomass occurs under light irradiation or thermal heating in solution with the production of reduced POM-I. Because POM-II has a much higher electrode potential (ca. 1.1 V, versus the normal hydrogen electrode (NHE)) compared to the reduced POM-I (ca. 0.3 V, versus NHE), the reduced POM-I releases electrons on the graphite-felt anode to POM-II in the cathode solution, which corresponds to steps 2 and 3. In the cathode tank, because the redox potential of POM-II is lower than oxygen (1.23 V, versus NHE), POM-II regeneration occurs by oxygen oxidation the step 4. As a result, the net reaction of the fuel cell is oxidation of biomass by O_2 to produce electricity.

The performance of LCFC powered by various biomasses is shown in Figure 2 A. Experimentally, 0.3 mol L^{-1} POM-I solution was mixed with biomass in the anode tank and 0.3 mol L^{-1} POM-II solution was filled in the cathode tank. It should be noted that some biomasses, such as grass powders, were particle suspensions in POM solution at the beginning. After preheating of POM-I in the anode tank at 100 °C for 4 h, the biomass was depolymerized to water-soluble fragments. Meanwhile, the color of the POM-I solution changed from yellow to deep purple (shown in Figure S2), illustrating the reduction of POM-I. The electrolyte solution readily generated electric current in the fuel cell when the external circuit was connected. As shown in Figure 2 A, the power densities were 22 and 34 mW cm^{-2}, respectively, when cellulose and starch were used as fuels. The power output of direct cellulose fuel cell is almost 3000 times higher than that the cellulosic microbial fuel cell.[12] Dry switchgrass powder and freshly collected plants (bush allamanda) were also used as the fuels. The power densities even reached 43 and 51 mW cm^{-2}, respectively.

The continuous operation of a cell directly fueled by starch was also conducted under a constant discharge current of 160 mA cm^{-2} (Figure 2 B; details are given in the Supporting Information). The cell worked continuously for more than 10 h under 80 °C and the power density was stabilized at approximately 30 mW cm^{-2}, which suggests both POM-I and POM-II are regenerated under these experimental conditions, and the biomass fuel cell can continuously provide electricity by directly consuming starch.

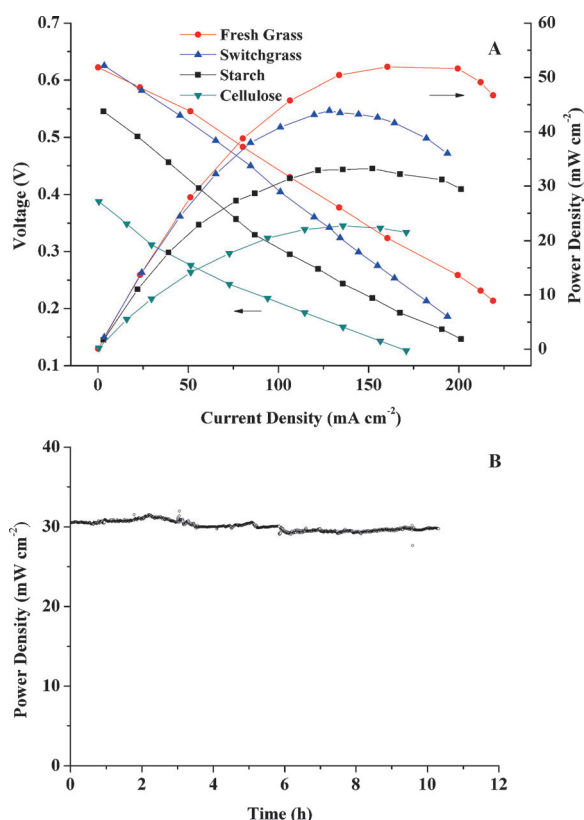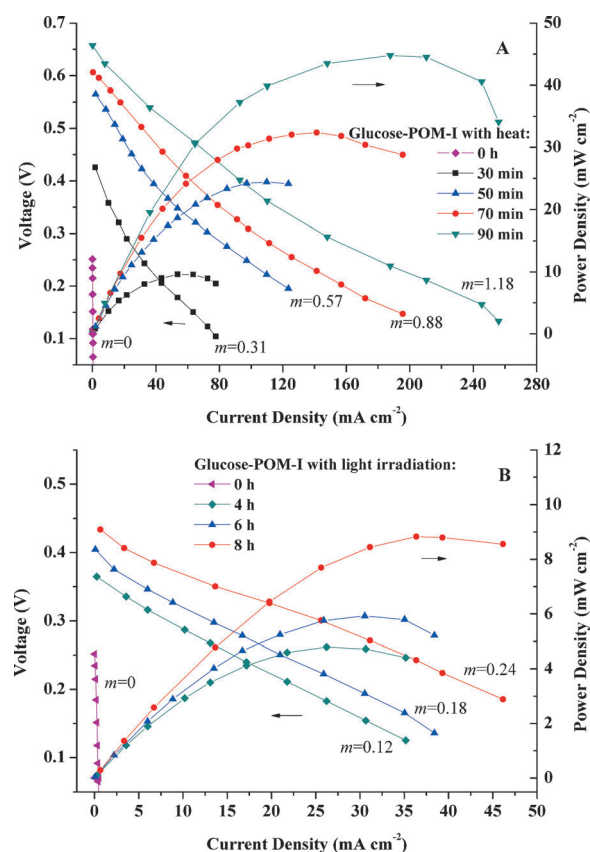of POM-II was realized by redox oxidation of oxygen in an oxygen-mixing tank.

In traditional fuel cells, oxygen reduction and hydrogen oxidation reactions occur directly on the catalyst surface. However, owing to the limited gas diffusion, fuel-cell electrodes are commonly 15–65 μm thick, the performance decays with thicker electrode.[11] In our fuel cell, both fuel oxidation (anode) and oxygen reduction (cathode) are catalyzed in POM solutions. Because H$^+$ ions can diffusion easily in water solution, as shown in Figure 1 A, both anode and cathode can be built as 3D electrodes and extended to several centimeters. It should be noted that, in traditional fuel cells, the noble-metal catalyst and conductive electrodes are coated on Nafion membranes. An increase in the electrode area means an increase of both the amount of expensive noble metal and membrane. However, for the liquid-catalyst fuel cell reported herein, the carbon electrodes are separated from the membrane. Therefore, the number of the carbon electrodes can be varied independently. By increasing the carbon electrode number in both the anode and cathode, the charge-transfer capacity will be increased, eventually the fuel cell can reach the maximum charge transfer capacity of the Nafion membrane. Furthermore, because carbon electrodes are extremely cheap, the increase in the carbon electrode number almost does not increase the total cost of the fuel cell but the power

Figure 2. A) Voltage–current-density and power–current-density plots for different biomasses at 80°C. The initial reduction degree of POM-**II** was 1.4 for all biomass-POM solutions. B) Power-density curve in continuous operation of the direct biomass fuel cell at 80°C for 10 h. The anode is a 50 mL starch-POM-**I** solution with a POM-**I** concentration of 0.3 mol L^{-1} and initial reduction degree 1.2; the cathode is 50 mL 2 Na-substituted POM-**II** solution with a concentration of 0.3 mol L^{-1}, reduction degree 1.6.

Figure 3. A) Voltage–current-density and power–current-density plots for glucose–POM-**I** reaction system with different reaction times at elevated temperature (100°C). The reduction degree (*m*) of POM-**I** at different reaction times is noted. The reduction degree of the initial POM-**II** solution at the cathode is 1.1; power density was measured at 80°C. B) Plots for the glucose–POM-**I** reaction system with different light irradiation times. The reduction degree of POM-**I** is noted; the initial reduction degree of POM-**II** and the operating temperature is the same as in (A).

The results clearly demonstrated that the new fuel cell design is able to provide high power density by simply preheating the biomass–POM solutions, however, the real redox reactions strongly depend on the nature of biomasses. For example, the oxidation reactions of starch are different from switchgrass. To understand the basic working mechanism of the anode, glucose that has a simple chemical structure was used as a model compound. Further experiments reveal that the LCFC performances are closely related to the reduction degree of the POM reacting with the biomass. Reduction degree, denoted as *m*, was defined as the number of mole of electrons accepted by one mole of POM. Because the reduced POM-**I** has a dark purple color, UV/Vis spectrophotometry is used to determine the reduction degree of POM-**I** based on changes in the intensity of the band at 510 nm (Figure S3).

As shown in Figure 3 A, with glucose-POM-**I** system held in the anode tank at 100°C, the reduction degree kept increasing. Correspondingly, the power density of the fuel cell output was raised from 9.5 to 45 mW cm^{-2} with the increase of POM-**I** reduction degree from 0.31 to 1.18 mole electron per mole POM after 90 min. This was further confirmed by using ascorbic acid, known as an active reductant. The reduction

degree reached 1.6 and the power density was as high as 90 mW cm^{-2} (Figure S4). Besides simple heating, the sunlight-induced glucose-powered fuel cell was also studied. Figure 3 B shows that with sunlight irradiation (AM-1.5 simulated sunlight), the reduction degree of POM-**I** gradually increased up to 0.24 and the power density reached 8.8 mW cm^{-2}. However, without light irradiation or heating, the power output was very low as expected because the POM-**I** reduction could not occur.

Although many factors could affect the power density of the fuel cell, the reduction degree of POM is one of the significant factors. The reason is Mo^{5+} in reduced POM-**I** releases electrons to the anode and determines the electrode potential, but oxidized biomass will not (Figure S5). As shown in Figure 4 A, anode electrode potentials drop from 0.8 V (vs. NHE, on graphite) to 0.35 V with the POM-**I** reduction degree increasing from 0 to 1.2. For the cathode electrolyte, POM-**II** had a high initial redox potential value of 1.09 V (vs. NHE, on graphite). Unlike the anode, the formal electrode potential of POM-**II** showed only a small drop when the reduction degree of POM-**II** was increased, because POM-**II**
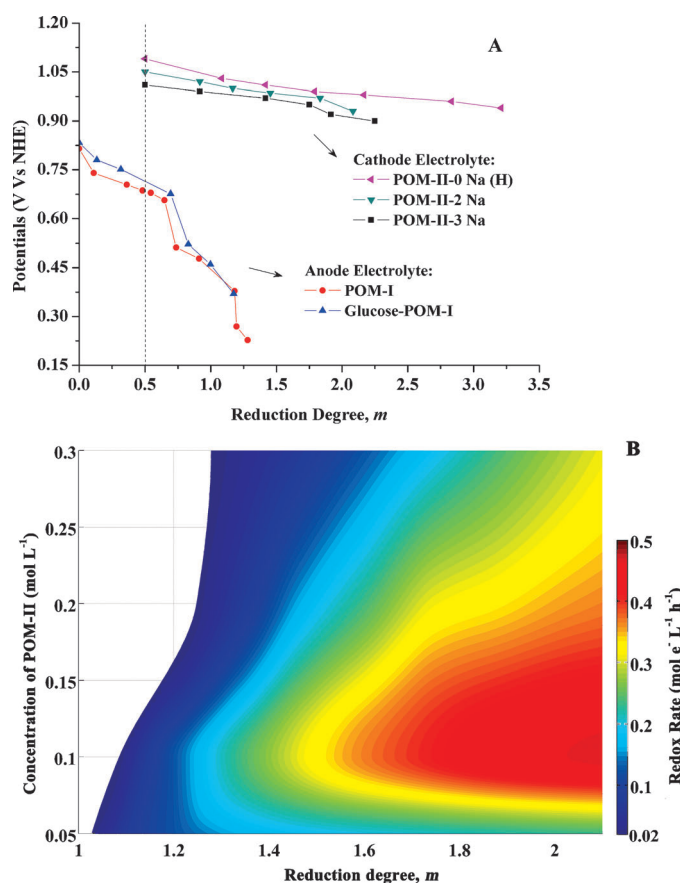
Figure 4. A) Electrode potentials of POM-**II** (0.3 mol L^{-1}) and glucose (2 mol L^{-1}) POM-**I** (0.3 mol L^{-1}) electrolyte as a function of reduction degree. POM-**II**-2 Na has two sodium-substituted POM-**II** and so forth. The potentials were measured in a single compartment set-up at room temperature, with a graphite working electrode and Ag/AgCl reference electrode. The value was recalculated based on normal hydrogen electrode (NHE). B) The redox rates (corresponded to different color) of oxygen and 2 Na substituted POM-**II** solution with different concentration and reduction degree. The results were obtained at 80°C and 1 atm oxygen pressure which are kept as a constant in this study.

is composed of seven vanadium atoms that act as a "vanadium reservoir" to maintain a relatively high redox potential during the discharge process. Therefore, as the reduction degree of POM-**I** increases, the voltage difference between anode POM-**I** and cathode POM-**II** increases as does the fuel-cell power output.

The redox reaction rate between POM-**I** and glucose was further investigated to estimate its capacity of donating electrons.

The number of electron transfers from glucose to POM-**I** at 100°C (shown in Figure S3) linearly increases with the reaction time, which is accordance with the literature.[13] The results evidently demonstrate that the redox reaction is zero order with respect to POM-**I**, suggesting that the reaction rate is constant at various reduction degrees of POM-**I**.

The redox reaction between POM-**II** and oxygen is complicated (shown in Figure S6) and associated with several factors, such as the acidity of solution, reduction degree and concentration of POM-**II**. The redox rate dramatically increased with the decrease of acidity of POM-**II** solution

(Figure S7). Zhizhina et al. reported that heteropoly acid solutions with lower acidity have an inherently faster oxygen oxidation rate than those with higher acidity.[14] Figure 4B shows the oxygen oxidation rate of 2 Na substituted POM-**II** at different reduction degrees and concentrations of POM-**II**. Different colors from blue to red in Figure 4B correspond to the values of redox rate from 0.02 to 0.5 mol e$^-$ L^{-1} h^{-1}. It can be seen that at a fixed concentration, the redox rate rapidly increases with reduction degree. However, at a fixed reduction degree the redox rate decreases as the concentration of POM-**II** increases from 0.1 to 0.3 mol L^{-1}, owing to the intrinsic acidity increase in a higher POM-**II** concentration. These results show that the POM catalyst have a sufficient reaction rate with biomass and oxygen to support the high-performance discharge.

During the POM catalytic oxidation, biomass is gradually decomposed, which is confirmed by the gel permeation chromatography (GPC) test in corn-starch-powered fuel cell (Figure S8). GPC can determine the molecular weight distribution of a polymer. The results show polymeric starch was degraded to small-molecular-weight species during the oxidation-discharge cycles. Oxidation products of the model compound glucose with POM-**I** were investigated by ^{1}H and ^{13}C NMR spectroscopy (Figure S9): They mainly consist of formic acid with minor amounts of glycolic acid, acetic acids and 5-hydroxymethyl furaldehyde (5-HMF). This indicates that the oxidation pathway of glucose (Figure S10) in our fuel cell is essentially the same as reported in literature.[15] The intermediate products can be further oxidized to CO$_2$ (Table S1). Total organic carbon (TOC) analysis shows that after repeated oxidation cycles, 88% of the initial glucose, 82% of the cellulose, and 65% of the lignin were converted into CO$_2$ (Figure S11). On the other hand, the biomass fuel can be completely degraded to CO$_2$ under light irradiation as measured in our photodegradation experiments with various sorts of biomass, including glucose, hemicellulose (xylan in this work), cellulose and lignin (shown in Figure S12), and as reported in the literature.[16] As one important part of discharge efficiency, Faradic efficiency in this fuel cell reaches 92.4% (Figure S13), which means that 92.4% of the total electrons released from the biomass in the anode travels to the cathode as external current.

As many alcohol fuel cells are working at elevated temperature (60–90°C),[17] our fuel cell is kept at a constant 80°C for the POM-catalyzed reactions. Although the pre-heating of the solution needs additional thermal energy, this energy input is mainly to cover the heat loss of the fuel cell, to maintain the fast reaction rate, so the conditions are similar to those used in most alcohol fuel cells. Actually, the biomass oxidation is intrinsically exothermic so no heating energy is required for the chemical reaction except to accelerate the reaction rate. Even for the small laboratory fuel cell used in this study, the thermal energy applied is much less than the electric energy obtained. Therefore, this fuel cell is an efficient biomass energy generator.

In summary, we demonstrated a new noble-metal-free fuel cell that can directly consume natural biomass at low temper-

ature and provides a large power density. The designed LCFC in this study incorporates photocatalysis and the thermal degradation of biomass in a single process. In essence, it is a hybrid of fuel cell and redox flow battery, which combines the advantages of both. The adopted POM catalyst is tolerant to catalyst-poisoning contaminants because POMs are robust and self-healing.[18] As a result, the biomass fuels do not require pre-purification treatment, which would significantly reduce the fuel cost. The principle of using POM liquid and carbon as the cathode can also provide a new method to other PEMFC systems.

Experimental Section

The flow-field plates of the fuel cell were made of high-density graphite plates with a serpentine flow channel (total geometry projected area of 1 cm²). A Versa Stat 3 electrochemical working station (Princeton Applied Research) was used to examine the *I–V* curves using the controlled potentiostatic method. Full experimental details are provided in the Supporting Information.

[1] C. Bianchini, P. K. Shen, *Chem. Rev.* **2009**, *109*, 4183–4206.
[2] J.-H. Wee, *Renewable Sustainable Energy Rev.* **2007**, *11*, 1720–1738.
[3] a) C. Lamy, E. M. Belgsir, J. M. Léger, *J. Appl. Electrochem.* **2001**, *31*, 799–809; b) A. Brouzgou, A. Podias, P. Tsiakaras, *J. Appl. Electrochem.* **2013**, *43*, 119–136.
[4] C. Bianchini in *Interfacial Phenomena in Electrocatalysis*, Vol. 51 (Ed.: C. G. Vayenas), Springer, New York, **2011**, pp. 203–253.
[5] M. Lefèvre, E. Proietti, F. Jaouen, J.-P. Dodelet, *Science* **2009**, *324*, 71–74.
[6] G. Wu, K. L. More, C. M. Johnston, P. Zelenay, *Science* **2011**, *332*, 443–447.
[7] a) D. Pant, G. Van Bogaert, L. Diels, K. Vanbroekhoven, *Bioresour. Technol.* **2010**, *101*, 1533–1543; b) A. Choudhury, H. Chandra, A. Arora, *Renewable Sustainable Energy Rev.* **2013**, *20*, 430–442.
[8] L. Yang, S. Wang, K. Blinn, M. Liu, Z. Liu, Z. Cheng, M. Liu, *Science* **2009**, *326*, 126–129.
[9] F. Ahmad, M. N. Atiyeh, B. Pereira, G. N. Stephanopoulos, *Biomass Bioenergy* **2013**, *56*, 179–188.
[10] L. Wei, M. Wei, L. Mengjie, Z. Xiaodan, C. Hongli, D. Yulin, *Nat. Commun.* **2014**, *5:3208*.
[11] a) S. Park, J.-W. Lee, B. N. Popov, *Int. J. Hydrogen Energy* **2012**, *37*, 5850–5865; b) U. Pasaogullari, C. Y. Wang, *J. Electrochem. Soc.* **2004**, *151*, A399.
[12] K. P. Gregoire, J. G. Becker, *Bioresour. Technol.* **2012**, *119*, 208–215.
[13] E. Papaconstantinou, *Z. Phys. Chem.* **1977**, *106*, 283–294.
[14] E. G. Zhizhina, V. F. Odyakov, M. V. Simonova, K. I. Matveev, *Kinet. Catal.* **2005**, *46*, 354–363.
[15] a) J. Tian, J. Wang, S. Zhao, C. Jiang, X. Zhang, X. Wang, *Cellulose* **2010**, *17*, 587–594; b) W. Deng, Q. Zhang, Y. Wang, *Dalton Trans.* **2012**, *41*, 9817–9831.
[16] A. Mylonas, A. Hiskia, E. Papaconstantinou, *J. Mol. Catal. A* **1996**, *114*, 191–200.
[17] M. Z. F. Kamarudin, S. K. Kamarudin, M. S. Masdar, W. R. W. Daud, *Int. J. Hydrogen Energy* **2013**, *38*, 9438–9453.
[18] M. T. Pope, A. Müller, *Angew. Chem. Int. Ed. Engl.* **1991**, *30*, 34–48; *Angew. Chem.* **1991**, *103*, 56–70.